JOURNAL OF CATALYSIS 103, 115–125 (1987)

Site Energy Distribution and Catalytic Properties of Microporous Crystalline $AlPO_4$-5

VASANT R. CHOUDHARY[1] AND DEEPAK B. AKOLEKAR

Chemical Engineering Division, National Chemical Laboratory, Pune 411 008, India

Received January 16, 1986; revised July 17, 1986

The site energy distribution on crystalline molecular sieve $AlPO_4$-5 (studied by temperature-programmed desorption of pyridine at different initial sorbate loadings and stepwise thermal desorption of the base from 373 to 673 K) has been found to be very broad. $AlPO_4$-5 possesses a significant catalytic activity in cracking of hydrocarbons (viz. cumene, *n*-hexane, isooctane, and butyl benzene isomers), isomerization of *o*-xylene and disproportionation of toluene, and also in conversion of methanol and ethanol to aromatics at 673 K. However, the catalytic activity in the above reactions varies significantly with the pulse number due to the coke deposition, which has both detrimental and beneficial effects on the catalytic processes. $AlPO_4$-5 contains both Lewis and protonic acid sites. The acid sites (particularly the protonic ones) are responsible for its catalytic activity. However, its strong acid sites are very small in number as compared to those on zeolites. The crystalline microporous aluminophosphate ($AlPO_4$-5) possesses much higher acidity and catalytic activity than the amorphous aluminophosphate.

INTRODUCTION

Recently, Wilson *et al.* (*1, 2*) have introduced a new class of crystalline aluminophosphate molecular sieves, which are similar to zeolites in many properties, and $AlPO_4$-5 belongs to this class. The crystal structure of $AlPO_4$-5 has been well established (*3*). It has a novel three-dimensional structure with hexagonal symmetry (cell constants $a = 1.373$ nm, $c = 0.848$ nm, and $\gamma = 120°$; unit cell composition 12 $AlPO_4 \cdot nH_2O$) and contains one-dimensional channels (pore diam. = 0.8 nm) oriented parallel to the *c*-axis and bounded by 12-membered rings composed of alternating AlO_4 and PO_4 tetrahedra. The axis in $AlPO_4$-5 is crystallographically polar (*3*). The polar nature of its structure is expected due to the vertical alignment of P—O—Al bonds in one direction caused by the strict up–down alternation of all the tetrahedra. $AlPO_4$-5 has neutral frameworks with no extra framework cations. However, it has a polar pore system consisting of the unidimensional cylindrical channels of uniform cross section. It is interesting to know the active sites and the catalytic properties of this crystalline microporous aluminophosphate.

Pyke *et al.* (*4*) have reported the chemical modification of $AlPO_4$-5 and catalytic properties of the modified $AlPO_4$-5. But no detailed information is available on the site energy distribution and catalytic properties of $AlPO_4$-5. The present work was undertaken with objective of investigating these properties of $AlPO_4$-5.

EXPERIMENTAL

Preparation and Characterization of $AlPO_4$-5

$AlPO_4$-5 was obtained from Pr_3N–$AlPO_4$-5 by removing the organic template (tripropylamine) from the latter by heating it in air at 823 K for 12 h (the temperature was raised at a heating rate of about 10 K min^{-1}). The Pr_3N–$AlPO_4$-5 was synthesized according to the hydrothermal procedure outlined by Wilson *et al.* (*5*) by crystallizing it from a gel of composition: 1.5 Pr_3N (tri-

[1] To whom all correspondence should be addressed.

0021-9517/87 $3.00

propylamine) · 1.0 Al_2O_3 · 1.0 P_2O_5 · 40 H_2O, at 423 K for 24 h. The source of Al_2O_3 and P_2O_5 was boehmite (Al · O · OH) and orthophosphoric acid (BDH AnalaR), respectively. The crystals of the aluminophosphate were washed thoroughly with deionized distilled water, filtered, and dried in an air oven at 373 K for 16 h.

The calcined aluminophosphate was pressed without any binder and crushed to 0.2–0.3 mm size particles.

The powder XRD spectrum (obtained by Holland Philips PW/1730 X-ray generator with the Ni-filtered CuKα radiation source and a scintillation counter) of the aluminophosphate was very similar to that for $AlPO_4$-5, reported earlier (*2*). The XRD data are given in Table 1.

The size and morphology of the crystals of the aluminophosphate were studied with a Cambridge Stereoscan Model 150 scanning electron microscope. The scanning electron micrograph of the aluminophosphate is shown in Fig. 1. The micrograph shows that the aluminophosphate is well crystallized and the crystals have a distinctly hexagonal cross section. The size of the hexagonal rod-like crystals is about 22 μm.

The chemical analysis showed that the Al/P ratio of the aluminophosphate is 1.03.

Amorphous aluminophosphate (Al/P = 1) was prepared by reacting aluminum trihydroxide with orthophosphoric acid. It was calcined in air at 823 K for 12 h.

TABLE 1

X-Ray Powder Diffraction Data for the $AlPO_4$-5

d (Å)	I/I_0 (%)	d (Å)	I/I_0 (%)	d (Å)	I/I_0 (%)
11.80	100	3.96	65	2.66	4
6.82	15	3.57	3	2.60	11
5.93	9	3.43	24	2.42	3
4.50	34	3.07	13	2.39	8
4.24	44	2.97	17		

FIG. 1. Scanning electron microphotograph of the $AlPO_4$-5.

Measurement of Site Energy Distribution

The site energy distribution of the aluminophosphate was measured by temperature-programmed desorption (TPD) of pyridine at the different initial sorbate loadings and also by stepwise thermal desorption (STD) of pyridine using a Perkin–Elmer Sigma 3B gas chromatograph fitted with a flame ionization detector. Nitrogen (>99.99%) passed over activated molecular sieves was used as a carrier gas.

A catalyst column was prepared by packing 0.42 g of the aluminophosphate (particle size: 0.2–0.3 mm) in a stainless-steel tube (i.d. 2 mm, o.d. 3 mm, and length 17 cm). One end of the column was directly connected to the detector and the other end to the injection block through a 55-cm-long stainless-steel capillary (i.d. 0.7 mm, o.d. 1.5 mm), which also acted as a preheater. Prior to the measurements the aluminophosphate was heated at 673 K for 2 h in the flow of nitrogen (10 $cm^3 \cdot min^{-1}$).

TPD. The TPD data were collected under the following experimental conditions: amount of the aluminophosphate, 0.42 g; N_2 flow rate, 10 $cm^3 \cdot min^{-1}$; initial temperature, 323 K; final temperature, 673 K; initial concentration of pyridine chemisorbed varied from 7.5 to 250 $\mu mol \cdot g^{-1}$; and linear heating rate, 10 K · min^{-1}. The amount of

pyridine chemisorbed measured by the TPD under the chromatographic conditions using the GC pulse technique (*6*) at 673 K was found to be 2.5 μmol · g^{-1}. The experimental procedure for the TPD experiments was similar to that described earlier (*7, 8*) except that the initial sorbate loading, in the present case, was varied by chemisorbing the base at different temperatures (>423 K). Thus at the start of the TPD, the sorbate was uniformly distributed on the sites of the aluminophosphate.

The advantages of using the GC technique with a catalyst packed in a long column (with a small diameter) over the conventional TPD technique (*9*) have been discussed before (*10*).

STD. The STD of pyridine was carried out by desorbing the base chemisorbed at 373 K on the aluminophosphate in the flow of nitrogen (10 cm^3 · min^{-1}) by heating it from 373 to 673 K in a number of steps. The temperature in each step was raised at a linear heating rate of 10 K · min^{-1}. After the maximum temperature of the respective step was attained, it was maintained for a period of 1 h to desorb the base reversibly sorbed in the aluminophosphate at that temperature. A detailed procedure for the STD experiments is given elsewhere (*8, 11*).

IR spectra of chemisorbed pyridine. IR spectra of pyridine chemisorbed on the $AlPO_4$-5 at different temperatures were taken at room temperature (301 K) using a Pye Unicam SP300 IR spectrophotometer.

Measurement of Catalytic Activity

The catalytic activity of the crystalline ($AlPO_4$-5) and amorphous aluminophosphates in the cracking of cumene, *n*-hexane, isooctane and butyl benzene isomers, disproportionation of toluene, isomerization of *o*-xylene, and conversion of methanol and ethanol to hydrocarbons was determined in a pulse microreactor (i.d. 4 mm) connected to the gas chromatograph, as a function of the pulse number, under the following conditions: amount of catalyst, 0.1 g; N_2 flow rate, 60 cm^3 · min^{-1}; temperature, 673 K; pulse size, 2.0 μl; total pressure, 180 kPa. Before the activity test, the catalyst was heated in the flow of nitrogen at 673 K for 2 h.

The catalytic activity in the cracking of *n*-butyl benzene, sec-butyl benzene, and tert-butyl benzene on the aluminophosphate poisoned by pyridine (chemisorbed at 723 K) was also measured.

The reaction products were analyzed on a column of Bentone-34 (5%) and dinonylphthalate (5%) on Chromosorb-W (3 mm × 9m) (carrier N_2; flow rate 20 cm^3 · min^{-1}); the column temperature was programmed from 323 to 438 K at a heating rate of 10 K · min^{-1}, while keeping the initial and final temperatures for 5 and 25 min, respectively.

The details of the microreactor and the procedure for measuring catalytic activity and for the catalyst poisoning are given in Refs. (*11, 12*).

The extent of coke deposition on the $AlPO_4$-5 in the catalytic reactions was determined by analyzing the coked $AlPO_4$-5 for carbon by microanalysis.

RESULTS

TPD of Pyridine

The TPD chromatograms on the $AlPO_4$-5 at different initial concentrations (θ_i) of pyridine are presented in Fig. 2. There is only one peak for the desorption, which indicates the involvement of only one type of active site in the desorption process. The desorption appears to be first order as the chromatograms are asymmetric. The peak maximum temperature (T_m) for the desorption is shifted toward the higher temperature side with the decrease in the value of θ_i, which indicates the presence of site energy distribution on the aluminophosphate. The values of T_m at different initial sorbate loadings are given below.

θ_i (μmol · g^{-1})	7.50	12.0	17.8	28.5	53.0	130	250
T_m (K)	633	613	585	563	520	510	507

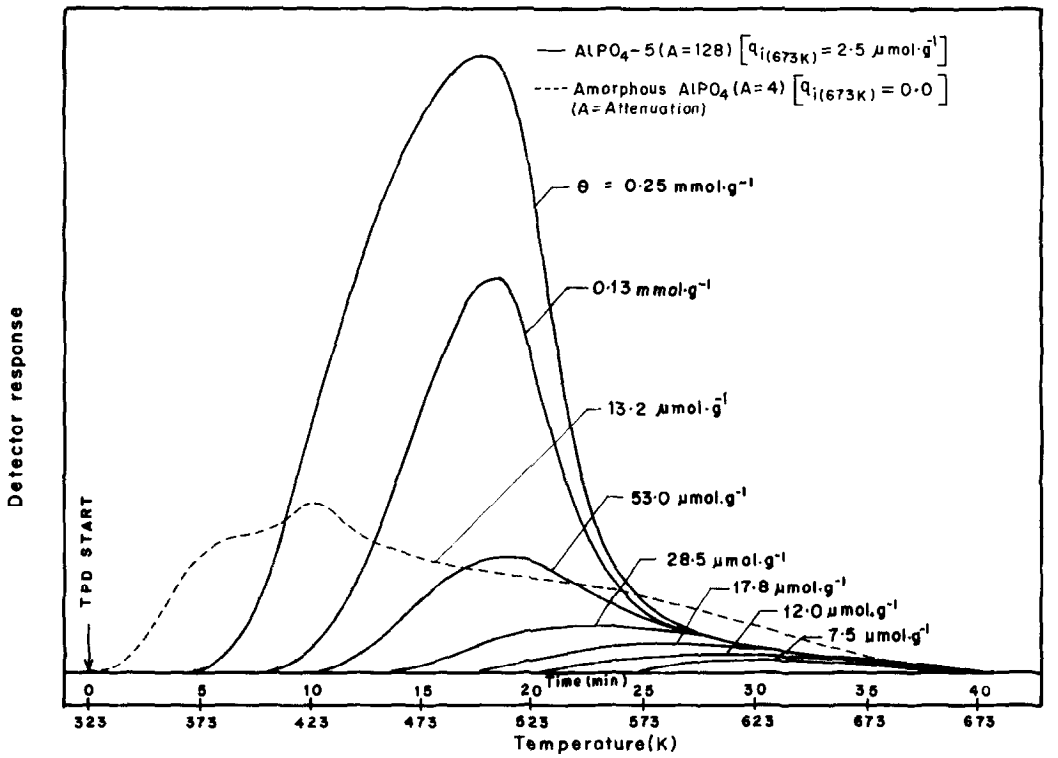

FIG. 2. TPD chromatograms of pyridine on the $AlPO_4$-5 and amorphous $AlPO_4$ (amount of catalyst, 0.42 g; N_2 flow rate, 10 $cm^3 \cdot min^{-1}$; heating rate, 10 $K \cdot min^{-1}$).

STD of Pyridine

The site energy distribution obtained from the STD of pyridine on the $AlPO_4$-5 is shown in Fig. 3b. The strength of the site involved in the pyridine chemisorption is expressed in terms of the desorption temperature (T_d), which lies in the range of temperatures in which the chemisorbed pyridine is desorbed. Here, T_d is the measure of the maximum strength possessed by the site and corresponds to the temperature at which the pyridine chemisorbed on the strongest site is desorbed. The columns in Fig. 3b show the strength distribution of the sites (equivalent to 1.12 mmol $\cdot$ g^{-1}) involved in the chemisorption at the lowest temperature of the STD (i.e., 373 K). The sites of strength 673 K $< T_d \leq T_d^*$ were obtained from the amount of pyridine chemisorbed at 673 K. On the other hand, the sites of strength $T_1 < T_d \leq T_2$ were obtained from the amount of pyridine, which was initially chemisorbed at T_1 but desorbed by increasing the temperature to T_2.

Figure 3a shows the temperature dependence of the chemisorption of pyridine on the aluminophosphate. The chemisorption data were obtained from the STD data by the procedure described earlier (*8, 11*). The chemisorption of pyridine at higher temperatures points to the involvement of the stronger sites. The q_i vs T curve, therefore, presents a type of site energy distribution in which the number of sites are expressed in terms of the amount of pyridine chemisorbed as a function of the sorption temperature.

In this study, the chemisorption is considered as the amount of pyridine retained by the presaturated aluminophosphate after it was swept with pure nitrogen for a period of 1 h and it is assumed that one site is involved in the chemisorption/desorption of one pyridine molecule.

IR Spectra of Chemisorbed Pyridine

The IR spectra of pyridine chemisorbed at 303 and 373 K on the $AlPO_4$-5 showed a significant absorbance at 1448 and 1545 cm^{-1}, which correspond (*13*) to coordinately bound pyridine and pyridinium ions, respectively. This indicated the presence of both Lewis and protonic acid sites on the aluminophosphate. The absorbance for the pyridine chemisorbed at 573 K was, however, found to be negligibly small as the number of strong acid sites on the aluminophosphates are very small.

Acidity of Amorphous Aluminophosphate

The chemisorption of pyridine on the amorphous aluminophosphate even at 373 K was found to be negligibly small. At 323 K it was only 13.2 $\mu mol \cdot g^{-1}$. A comparison of the TPD curves in Fig. 2 also shows that the amorphous aluminophosphate contains only a few weak acid sites.

Catalytic Activity in Hydrocarbon Cracking

The data on the catalytic activity and its variation with the pulse number for the

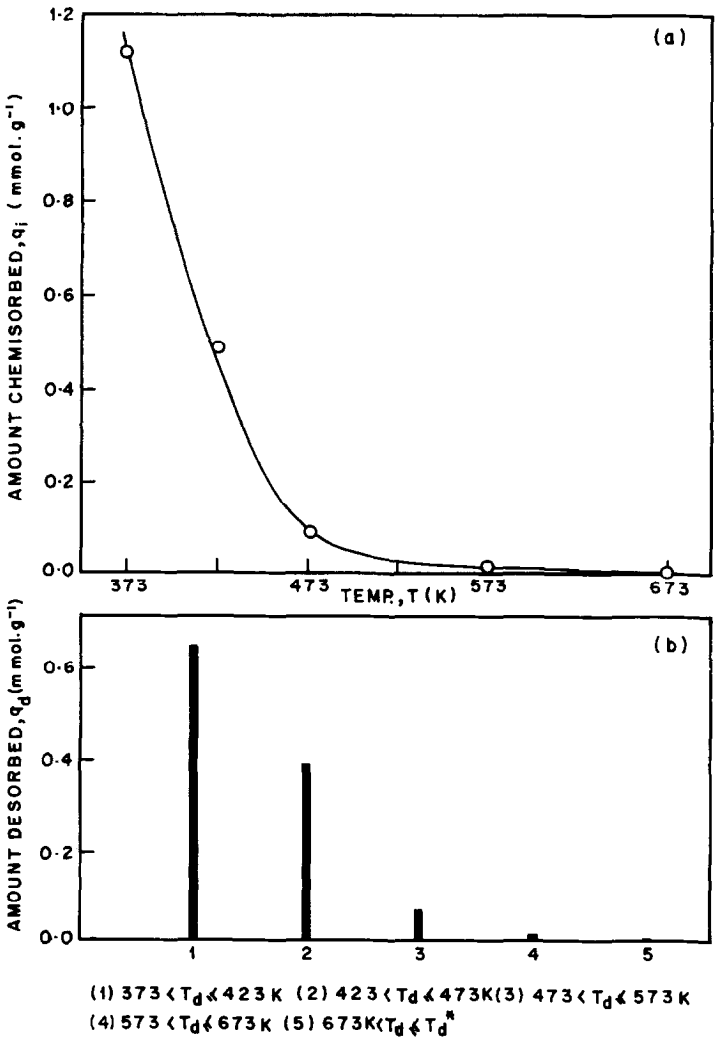

FIG. 3. (a) Temperature dependence of chemisorption of pyridine on the $AlPO_4$-5. (b) Site energy distribution on the $AlPO_4$-5 (obtained by the STD of pyridine from 373 to 673 K).

cracking of *n*-hexane, isooctane and cumene on the $AlPO_4$-5 are presented in Fig. 4. The catalytic activity in the cracking of the hydrocarbons is in the following order: cumene ≫ isooctane > *n*-hexane.

When the pulse number is increased from 1 to 20, the catalytic activity decreases continuously in the cumene cracking, increases in the isooctane cracking and passes through a maximum in the *n*-hexane cracking.

The cumene cracking activity lost in the pulse experiments could be regained after heating the deactivated $AlPO_4$-5 (after 50th pulse experiment) in a flow of N_2 (60 $cm^3 \cdot min^{-1}$) containing oxygen (5%) at 773 K for 12 h, indicating the regenerability of the catalyst. The deactivation is thus expected due to the coke deposition in the channels of the $AlPO_4$-5. The microanalysis showed that the concentration of carbon in the deactivated $AlPO_4$-5 was 1.83 (wt%).

The results of the cracking of butyl benzene isomers at 673 K on the fresh and poisoned $AlPO_4$-5 are given in Table 2. The aluminophosphate was poisoned by the chemisorption of pyridine at 723 K. On the poisoned aluminophosphate, its very strong sites (1.5 $\mu mol \cdot g^{-1}$) were blocked by the chemisorbed pyridine. The catalytic activity of the fresh and poisoned $AlPO_4$-5 in the cracking of the butyl benzene isomers is in the following order: tert-butyl benzene > sec-butyl benzene > *n*-butyl benzene. Due to the poisoning, the catalytic activity is decreased. The decrease in the activity is very small in the cracking of tert-butyl benzene but it is very pronounced in the cracking of *n*-butyl benzene.

TABLE 2

Data on the Cracking of Butyl Benzene Isomers on the Fresh and Pyridine Poisoned $AlPO_4$-5 at 673 K

Reactant	Conversion (%)	
	Fresh catalyst	Pyridine-poisoned catalyst
n-Butyl benzene	19.7	8.6
sec-Butyl benzene	88.7	81.1
tert-Butyl benzene	99.5	97.6

The amorphous aluminophosphate, however, showed a very small catalytic activity in the cumene cracking (0.5% conversion of cumene). It has not shown any activity in the cracking of *n*-hexane and isooctane.

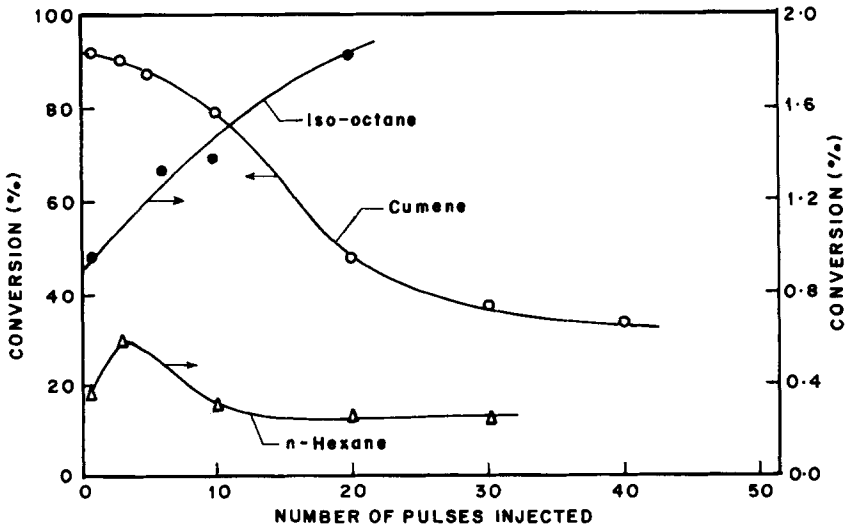

FIG. 4. Variation in the conversion of cumene, isooctane, and *n*-hexane on the $AlPO_4$-5 (at 673 K) with the pulse number.

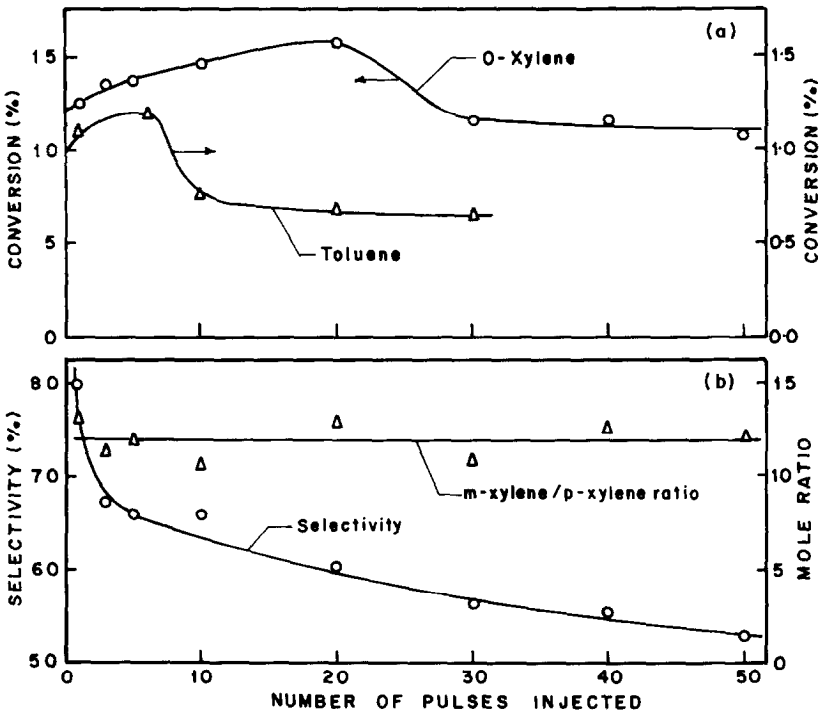

FIG. 5. (a) Influence of pulse number on the total conversion of *o*-xylene and toluene on the $AlPO_4$-5 at 673 K. (b) Dependence of the selectivity and *m*-xylene/*p*-xylene ratio in the isomerization of *o*-xylene on the pulse number.

Catalytic Activity in Isomerization and Disproportionation Reactions

The results of the isomerization of *o*-xylene and the disproportionation of toluene on the $AlPO_4$-5 are presented in Fig. 5. The total conversion of *o*-xylene and toluene (Fig. 5a) passes through a maximum and then attains a somewhat steady value with the increase in the pulse number. The conversion of toluene is very small, whereas the conversion of *o*-xylene is appreciable.

In the isomerization of *o*-xylene, with the increase in the pulse number from 1 to 50, the selectivity for the isomerization decreases very significantly but the *m*-xylene/*p*-xylene ratio remains almost the same. A formation of benzene and toluene to an appreciable extent was observed in the conversion of *o*-xylene. This indicates that along with the isomerization, disproportionation and dealkylation reactions also occur.

The amorphous aluminophosphate showed no activity in the above reactions.

Catalytic Activity in Alcohol-to-Aromatics Conversion

Figure 6 shows the results of the conversion of methanol and ethanol to hydrocarbons and the concentration of aromatics in the hydrocarbons formed on the $AlPO_4$-5 at 673 K as a function of pulse number. The initial activity of the $AlPO_4$-5 (i.e., the conversion in the first pulse experiment) in both alcohol conversion reactions is very high (nearly 100% conversion). However, the conversion decreases with the increase in pulse number, the decreases being more pronounced in the methanol conversion.

The conversion of ethylene (pulse size 1 cm^3) to higher hydrocarbons under the same experimental conditions was found to be negligibly small (<0.1%).

It is interesting to note that the formation

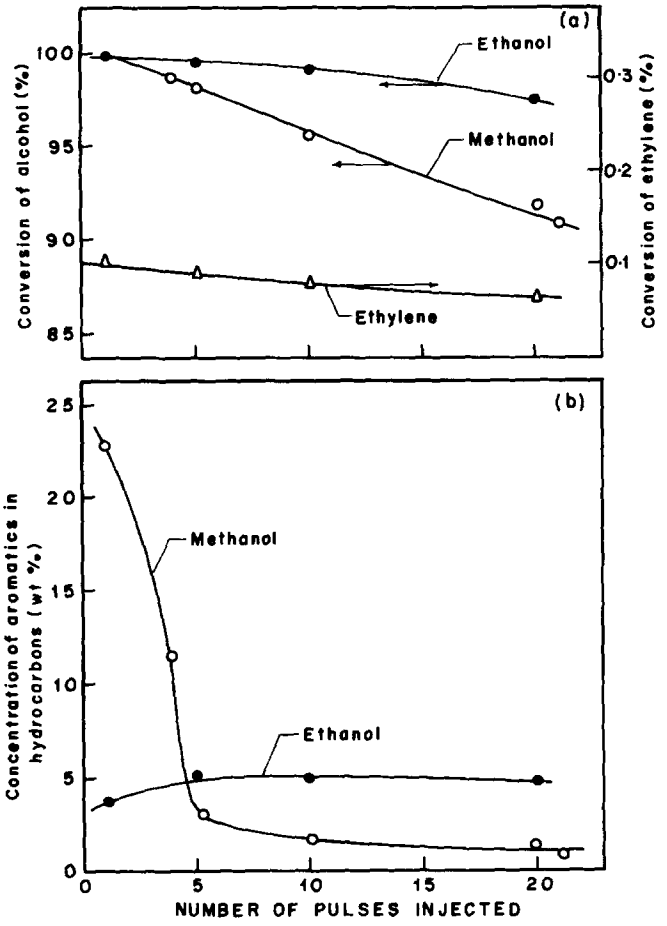

FIG. 6. (a) Variation of the converison of methanol, ethanol, and ethylene on the $AlPO_4$-5 with the pulse number. (b) Variation in the formation of aromatics in the conversion of methanol and ethanol at 673 K with the pulse number.

of aromatics in the converison of methanol decreases sharply with the increase in the pulse number. On the other hand, the aromatics formed in the conversion of ethanol was not affected very significantly by the increase in pulse number. It may also be noted that the initial aromatization activity of the $AlPO_4$-5 is much higher in the conversion of methanol than ethanol. The distribution of products (hydrocarbons) formed in the first pulse experiment in both the alcohol conversions is presented in Table 3. The formation of aromatics in the methanol conversion is in the following order: benzene > toluene > C_8-aromatics > C_{9+}-aromatics, whereas the order in the ethanol conversion is as follows: C_{9+}-aromatics > C_8-aromatics > benzene > toluene.

On the amorphous aluminophosphate, the conversion of methanol and ethanol was about 5 and 34%, respectively. There was no formation of aromatics.

DISCUSSION

Active Sites and Site Energy Distribution on $AlPO_4$-5

The results on TPD and STD of pyridine have clearly shown that there exists a site energy distribution on the $AlPO_4$-5 and the distribution is very broad. The $AlPO_4$-5 contains a very few strong sites and the ma-

TABLE 3

Distribution of Hydrocarbons in the Initial Conversion (i.e., in the First Pulse Experiment) of Methanol and Ethanol on the $AlPO_4$-5 at 673 K

Reactant	Concentration of hydrocarbons (wt%)	
	Methanol	Ethanol
Aliphatics	77.10	96.17
Benzene	10.50	0.58
Toluene	6.03	0.42
Ethyl benzene	0.97	0.02
p-Xylene	1.24	0.21
m-Xylene	1.02	0.26
o-Xylene	1.14	0.30
Total xylenes	(3.40)	(0.77)
C_{9+}-aromatics	2.00	1.90
Total aromatics	(22.90)	(3.69)
Total	100	100

Note. Conversion of methanol and ethanol = 100%.

jority of sites are weaker ones. The chemisorption of pyridine (which is a base having intermediate basicity, $pK_\alpha \simeq 5.2$), particularly at the higher temperatures, points to the existence of acid sites on the aluminophosphate. This is further confirmed by the catalytic activity shown by the aluminophosphate in the acid-catalyzed reactions, such as the cracking of the hydrocarbons (viz. cumene, *n*-hexane, isooctane and butyl benzene isomers), the isomerization of *o*-xylene, the disproportionation of toluene, and the aromatization in methanol and ethanol conversion reactions. The formation of coke, which itself is acid-catalyzed (*14*), also points to the presence of acid sites on the aluminophosphate. The IR spectroscopic study of chemisorbed pyridine has clearly indicated the presence of both Lewis and protonic acid sites on the $AlPO_4$-5. This is consistent with the observation made recently by Bond and co-workers (*15*) from their IR studies on $AlPO_4$-5. The occurrence of the above reactions indicates that the active sites on the aluminophosphate are mostly the protonic acid sites. Our recent studies (*16*) have also indicated that the catalytic activity of the $AlPO_4$-5 in the cumene cracking and *o*-xylene isomerization reactions decreases very significantly when its calcination temperature is increased from 823 to 1273 K. This provides an indirect proof for the involvement of protonic sites in the catalytic processes on $AlPO_4$-5.

It may be noted that though $AlPO_4$-5 contains acid sites, it possesses only a very few strong acid sites (measured in terms of the chemisorption of pyridine at 623 K) (7.5 μmol $\cdot$ g^{-1}) as compared to zeolites H-ZSM-5 [(Si/Al = 17.2), 0.34 mmol $\cdot$ g^{-1} (*11*); CeY, 0.42 mmol $\cdot$ g^{-1} (*8*); CeX, 0.5 mmol $\cdot$ g^{-1} (*17*); HY, 0.78 mmol $\cdot$ g^{-1} (*17, 18*); and H-mordenite, 0.77 mmol $\cdot$ g^{-1} (*18*)]. The presence of acidity is not expected from the composition of the $AlPO_4$-5. The origin of the acid sites is not clear and further work is essential for this purpose.

Catalytic Activity of the $AlPO_4$-5

The aluminophosphate possesses a high initial catalytic activity in the cracking of cumene, tert-butyl benzene, and sec-butyl benzene, as these reactions can also occur on weaker acid sites. The low activity in the cracking of *n*-butyl benzene, isooctane, and *n*-hexane is mostly due to the presence of only a few strong acid sites. The very significant decrease in the conversion of *n*-butyl benzene as compared to that in the conversion of tert-butyl benzene and sec-butyl benzene due to the poisoning of the aluminophosphate clearly points to the involvement of strong acid sites in the cracking of *n*-butyl benzene. Thus the results of the cracking of the butyl benzene isomers also indicates the presence of both the strong (which are fewer in number) and weak acid sites on the aluminophosphate. The $AlPO_4$-5 possesses an appreciable catalytic activity in the isomerization of *o*-xylene but somewhat poor selectivity due to simultaneous occurrence of dealkylation

and disproportionation reactions. The high *m*-xylene/*p*-xylene ratio (which is about 12) indicates that the formation of *m*-xylene is kinetically controlled [at equilibrium, *m*-xylene/*p*-xylene ratio (at 673 K) is about 2.2].

The toluene disproportionation activity of the aluminophosphate is very low (toluene conversion $\simeq$ 1%). The disproportionation and isomerization activity is consistent with what is expected from the availability of acid sites of different strengths; the isomerization occurs on the acid sites weaker than those involved in the disproportionation reactions (*12*).

The aluminophosphate also has a high activity in the conversion of methanol and ethanol to hydrocarbons; both the alcohols are almost completely converted in the first pulse experiment. Use of crystalline aluminophosphates in alcohol conversion is also reported in a recent U.S. Patent 4,524,234. A very low conversion of ethylene (<0.1%) to higher hydrocarbons points to the fact that the methanol-to-aromatics conversion does not involve the formation of ethylene as an intermediate or if ethylene is formed the further aromatization requires the presence of other reaction species formed from the alcohol. In the ethanol conversion process, the formation of ethylene is expected on the aluminophosphate and probably this may be the reason for the lower initial aromatization activity in the ethanol conversion as compared to that in the methanol conversion. The difference in the distribution of aromatics in the two alcohol conversion processes (Table 3) is expected mostly due to different reaction paths followed in the overall conversion. However, a detailed further investigation is necessary for arriving at the definite conclusion on this matter.

The decrease in the catalytic activity in the cumene cracking and the alcohol conversions is mainly due to coke deposition. The catalyst deactivation in the cracking and methanol conversion is very fast. It is expected mostly due to pore mouth poisoning (i.e., by the deposition of the coke at the channel entrance) because even at a low coke deposition (1.83% at the end of 50th pulse in the cumene cracking), the catalytic activity is dropped to a very significant extent (conversion of cumene dropped from 92 to 34%). Similar to mordenite (which contains unidimensional pore system), the $AlPO_4$-5 is expected to be deactivated very fast because of its unidimensional pore system.

The increase in the isooctane cracking activity and the aromatiation activity in the ethanol conversion and the maximum in the conversion of *n*-hexane, toluene, and *o*-xylene with the increase in the pulse number is mostly attributed to the catalytically active sites on the coke deposited in the previous pulse experiments. Earlier studies on zeolites (*14*) have also indicated the possibility of the existence of active sites (carbonium ions type) on coke, which can have both detrimental and beneficial effects on catalytic processes.

A comparison of the results on the $AlPO_4$-5 and the amorphous aluminum phosphate showed that the crystalline aluminophosphate has much higher catalytic activity.

CONCLUSIONS

The following conclusions have been drawn from the present study.

There exists a broad site energy distribution on the $AlPO_4$-5 which contains both Lewis and protonic sites. The catalytic properties of the $AlPO_4$-5 are attributed to the presence of acid sites, mostly protonic sites. However, the number of strong acid sites on the aluminophosphate are very few as compared to those on zeolites. The $AlPO_4$-5 possesses a significant catalytic activity in the cracking, isomerization, alcohol-to-aromatics conversion reactions. However, the catalytic activity varies significantly with the pulse number due to the coke deposition. Both the detrimental and beneficial effects of the coking (in the first few pulse experiments) have been ob-

served. Nevertheless, in general, the catalyst deactivation due to the coke deposition is very fast due to the unidimensional pore system of the aluminophosphate.

As compared to the amorphous aluminophosphate, the $AlPO_4$-5 possesses very high acidity and catalytic activity.

REFERENCES

1. Wilson, S. T., Lok, B. M., Messina, C. A., Cannan, T. R., and Flanigen, E. M., *J. Amer. Chem. Soc.* **104,** 1146 (1982).
2. Wilson, S. T., Lok, B. M., Messina, C. A., Cannan, T. R., and Flanigen, E. M., *ACS Symp. Ser.* **218,** 79 (1983).
3. Bennett, J. M., Cohen, J. P., Flanigen, E. M., Pluth, J. J., and Smith, J. V., *ACS Symp. Ser.* **218,** 109 (1983).
4. Pyke, D. R., Whitey, P., and Houghton, H., *Appl. Catal.* **18,** 173 (1985).
5. Wilson, S. T., Lok, B. M., Messina, C. A., and Flanigen, E. M., *in* "Proceedings, 6th Intl. Zeolite. Conf., Reno, July 10–15, 1983" (D. Olson and A. Bisio, Eds.), p. 97. Butterworth, Surrey, 1983.
6. Choudhary, V. R., and Nayak, V. S., *Appl. Catal.* **4,** 31 (1982).
7. Choudhary, V. R., *J. Chromatogr.* **259,** 283 (1983).
8. Choudhary, V. R., *J. Chromatogr.* **268,** 207 (1983).
9. Cvetanovic, R. J., and Amenomiya, Y., "Advances in Catalysis," Vol. 17, p. 103. Academic Press, New York, 1967.
10. Choudhary, V. R., *J. Chromatogr.* **157,** 391 (1978).
11. Nayak, V. S., and Choudhary, V. R., *J. Catal.* **81,** 26 (1983).
12. Nayak, V. S., and Choudhary, V. R., *Appl. Catal.* **4,** 333 (1982).
13. Parry, E. P., *J. Catal.* **2,** 371 (1963).
14. Derouane, E. G., *in* "Catalysis by Acids and Bases" (B. Imelik *et al.*, Eds.), p. 221. Elsevier, Amsterdam, 1985.
15. Bond, G. C., Gelsthrope, M. R., Sing, K. S. W., and Theocharis, C. R., *J. Chem. Soc., Chem. Commun.* **15,** 1056 (1985).
16. Choudhary, V. R., Akolekar, D. B., Sansare, S. D., and Singh, A. P., unpublished work.
17. Choudhary, V. R., Srinivasan, K. R., and Akolekar, D. B., *Zeolites*, in press.
18. Choudhary, V. R., *Zeolites*, in press.